

# Overstrength of I-Shaped Shear Links for EBF Design

Hyoung-Bo Sim, Xiao-Jun Fang, and Chia-Ming Uang

## ABSTRACT

Past experimental research on EBF indicated that the link overstrength, particularly that for short (i.e., shear) links, could be much higher than that specified in the AISC Seismic Provisions, thus potentially leading to an unsafe design of beams, columns, and gusset connections per the capacity design requirements. This study aims to identify key factors contributing to the high overstrength and to derive an expression to predict the overstrength of short links. Available experimental data were first collected, and main parameters affecting the overstrength were identified from the database and used for a multi-variate regression analysis. It was found that the following two parameters affect the link overstrength the most: (1) the  $F_u/F_y$  ratio between the actual tensile strength and yield stress and (2)  $K_w$ , a factor that represents the contribution of localized bending of link flanges. The link length, to a lesser extent, also affects the overstrength. A predictive overstrength equation based on these three parameters was proposed for capacity design of EBF with short links.

**KEYWORDS:** eccentrically braced frames, cyclic tests, link overstrength, seismic design.

## INTRODUCTION

Eccentrically braced frames (EBFs) combine the advantages of the high ductility of special moment frames and the high elastic lateral stiffness approaching that of concentrically braced frames (Roeder and Popov, 1978; Popov and Engelhardt, 1988; Bruneau et al., 2011). A typical EBF consists of links, braces, beams outside the links, columns, and connections. According to the AISC *Seismic Provisions*, ANSI/AISC 341 (AISC 2016, 2022a), hereafter referred to as AISC 341, links are designed to dissipate seismic energy, while structural components other than beams outside the link are designed to remain essentially elastic in a seismic event. (Because beams outside the link and the link itself are continuous and have the same section, it is difficult to keep the beams elastic without stiffening. Thus, AISC 341 allows these beams to experience limited flexural yielding.) Observed performance of actual EBF buildings in earthquakes is very limited in the United States. But experience from the 2010 and 2011 Christchurch, New Zealand, earthquakes did show good overall performance (Bruneau et al., 2010; Clifton et al., 2011).

The link rotation angle,  $\gamma_p$ , defined as the inelastic (or plastic) angle between the link and the beam outside of the link, is used to describe the inelastic deformation capacity of a link. The rotation angle is a function of the link length,  $e$ , which in turn dictates if it will yield primarily in shear, flexure, or a combination of the two (Roeder and Popov, 1978; Malley and Popov, 1984; Kasai and Popov, 1986; Okazaki and Engelhardt, 2007). Define the normalized link length,  $\rho$ , as

$$\rho = \frac{e}{M_p/V_p} \quad (1)$$

where  $M_p$  is the plastic moment and  $V_p$  is the plastic shear strength. When  $\rho \leq 1.6$  (i.e., short or shear links), AISC 341 specifies that a properly stiffened shear-yielding link has a link rotation angle capacity of at least 0.08 rad.

For capacity design of diagonal braces and brace connections, beams outside the link, and columns, the nominal shear strength of a link needs to be adjusted to reflect two effects: (1) actual yield strength of the steel and (2) other factors, including strain hardening and flange contribution under cyclic loading. AISC 341 uses an adjustment factor  $R_y$  to account for the first effect. For shear-yielding links, the second effect is quantified by defining an overstrength factor,  $\Omega_t$ , in this study:

$$\Omega_t = \frac{V_u}{V_{pa}} \quad (2)$$

where  $V_u$  represents the maximum shear strength measured in experimental testing (which is equivalent to the required shear strength in design) and  $V_{pa}$  is the plastic shear strength:

$$V_{pa} = 0.6F_{ya}(d - 2t_f)t_w \quad (3)$$

Hyoung-Bo Sim, Associate Professor, Department of Civil and Environmental Engineering, In.eon National University, In.eon, South Korea. Email: hbsim@inu.ac.kr

Xiao-Jun Fang, Graduate Student Researcher, Department of Civil and Environmental Engineering, In.eon National University, In.eon, South Korea. Email: fangxiaojun@inu.ac.kr

Chia-Ming Uang, Professor, Department of Structural Engineering, University of California, San Diego, La Jolla, Calif. Email: cmu@ucsd.edu (corresponding)

Paper No. 2022-04

ISSN 0013-8029

ENGINEERING JOURNAL / FIRST QUARTER / 2023 / 21

In Equation 3,  $d$ ,  $t_f$ , and  $t_w$  are the overall depth, flange thickness, and web thickness, respectively, and  $F_{ya}$  is the measured yield stress of the web. To avoid confusion,  $F_y$  and  $F_u$  refer to the minimum specified yield stress and tensile strength, respectively, in AISC 341, while the measured (or actual) yield stress and tensile strength are referred to as  $F_{ya}$  and  $F_{ua}$  in this study. If  $F_y$  were used in Equation 3, the computed  $\Omega_l$  value from Equation 2 would include both effects mentioned earlier. Because this study investigates the second effect (i.e., link overstrength), the measured yield stress,  $F_{ya}$ , from tensile coupon testing is used in Equation 3.

Based on test results of rolled wide-flange links of ASTM A36 steel in the 1980s, an overstrength factor of 1.5 for strain hardening was recommended (Popov and Engelhardt, 1988). Testing that was conducted after the 1994 Northridge, California, earthquake on rolled wide-flange links of ASTM A992 steel showed that the overstrength factor ranges from 1.05 to 1.62, with an overall average of 1.35 (Okazaki and Engelhardt, 2007). For short links dominated by shear yielding, the overstrength tends to be somewhat higher (1.25 to 1.62, with an average of 1.41). Note that all ASTM A36 or A992 steel links tested were rolled wide-flange shapes, and member sizes were small and not heavy; for example, W10×19, W10×33, W16×36, and W18×40 of ASTM A992 steel were tested by Okazaki and Engelhardt (2007).

To achieve an economical EBF design, AISC 341 has been specifying a lower overstrength factor (1.25) for I-shaped links for capacity design of columns, diagonal braces, and their connections. That is, the required seismic forces for these components are based on the assumption that the member forces at the ends of the link correspond to a link shear of 1.25 times the expected shear strength,  $R_y V_n$ . According to the Commentary in the 1997 edition of the AISC *Seismic Provisions*, this lower value was justified on the basis that, for brace design, the nominal yield strength and a resistance factor are used in sizing the braces; assuming that  $R_y$  is equal to 1.1 and the resistance factor is 0.9, the effective overstrength of the link is  $1.25 \times 1.1/0.9 = 1.53$ . The link overstrength factor is further relaxed from 1.25 to 1.1 for the design of beams outside the link because (1) beam strength will be enhanced by the presence of a composite slab, and (2) limited yielding in the beams is judged to be non-detrimental to the EBF performance (Commentary to AISC 341, 2016).

The discussion on link overstrength presented earlier applies to hot-rolled W-shape links. For I-shaped built-up links, however, available experimental data indicated that the overstrength factor can be significantly higher than that specified in AISC 341. For example, McDaniel et al. (2003) conducted cyclic tests of two large-size built-up shear links of ASTM A709 Gr. 50 steel to evaluate the link performance

for bridge applications; the reported values of the overstrength factor were 1.83 and 1.94, respectively. Itani et al. (2003) reported that the overstrength factor was about 1.80 based on cyclic testing of two built-up links of A709 Gr. 50 steel. Based on finite element simulation, Barecchia et al. (2006) proposed a formula to evaluate the overstrength factor of short and intermediate links with European hot-rolled shapes. The study found that the overstrength factor would increase with a reduced  $\rho$  and an increased  $b_f/d$  ratio, where  $b_f$  is the flange width. Ji et al. (2016) tested very short hybrid steel links, where the yield stresses of the web (33 to 41 ksi) are lower than that of the flanges, and the overstrength factor reached 1.9. The authors attributed this large overstrength to the contribution of link flanges and cyclic hardening of the web steel. Two large-size built-up shear links with ASTM A709 Gr. 50 steel were tested for building construction and, again, large overstrength was observed (Sim and Uang, 2011; Gulec et al., 2012).

Based on Richards and Uang (2006), the AISC 341 Commentary (AISC, 2016) states that designers should consider a high overstrength factor for large built-up links with very thick flanges and very short lengths ( $e < M_p/V_p$  or  $\rho < 1.0$ ). Azad and Topkaya (2017) provided a summary of past research, both analytical and experimental, on the overstrength factor of links and found it inconclusive that thick flanges are the main contributing factor for very high overstrength.

## OBJECTIVE AND SCOPE

There is no consensus on the cause and main contributing factors for the “unusual” high overstrength observed from testing of some short links. Because this would potentially produce an unsafe capacity design and AISC 341 does not provide any design guidelines, the goal of this study is to identify key contributing factors and to derive an expression to predict the overstrength of short links.

## EXPERIMENTAL DATABASE

The following criteria were used to establish the experimental database (see Table 1). First, only short links were selected because links that showed large overstrength in testing were classified per AISC 341 as short links. Therefore, only data with  $\rho$  no greater than 1.6 were considered. Table 1 shows that most of the specimens collected had  $\rho$  less than 1.1. Second, links with both rolled wide-flange and built-up I-shape sections were included. Third, only specimens that were tested after the 1994 Northridge, California, earthquake were considered because 36 ksi steel is much less likely to be used for new construction in the future. For rolled shapes, therefore, it means that only A992 steel was considered, and A36 steel was excluded in the

Table 1. Test Matrix for Regression Analysis of Link Overstrength Factors

Group No.	Steel Grade	Section	Specimen Designation	$\rho$	$F_{yb}$ (ksi)		$F_{ua}$ (ksi)		$b_f/2t_f$	$h/t_w$	$t_f/t_w$	$A_f/A_w$	$b_f/d$	$K_w$	$\Omega_f^a$	$\Omega_f^b$
					Web	Flange	Web	Flange								
1 Okazaki and Engelhardt (2007)	A992	W10x33	4A-RLP	1.04	51.6	55.4	73.5	73.0	9.2	28.4	1.50	1.23	0.82	0.070	1.45	1.32
			12-RLP	1.02	51.1	57.0	72.4	76.4	6.1	54.0	1.67	0.56	0.34	0.038	1.44	1.36
		W10x68	8-RLP	1.49	52.5	56.9	77.5	81.9	7.1	48.0	1.46	0.64	0.44	0.023	1.37	1.30
			10-RLP	1.25	46.3	58.6	69.5	77.0	6.6	17.8	1.64	1.59	0.97	0.100	1.47	1.25
2 Mansour et al. (2011)	A992	W10x33(B)	S9	0.99	55.0	58.3	75.1	76.9	9.2	28.4	1.50	1.23	0.82	0.070	1.43	1.30
			UT-3A	1.16	55.1	64.5	72.7	80.0	7.0	28.6	1.73	1.24	0.71	0.076	1.41	1.27
3 Dusicka et al. (2010)	A709 Gr. 50	Built-up I-section	UT-3B	1.16	55.1	64.5	72.7	80.0	7.0	28.6	1.73	1.24	0.71	0.076	1.42	1.28
			C345	0.83	56.6	54	78.7	73.9	6.8	31.0	1.57	0.99	0.63	0.078	1.90	1.72
4 Itani et al. (2003)	A709 Gr. 50	Built-up I-section	BU16	1.31	54.0	57.0	84.0	81.0	4.7	34.7	4.00	3.50	0.88	0.109	1.82	1.48
			BU30	1.31	54.0	57.0	84.0	81.0	4.7	54.0	3.00	1.40	0.47	0.044	1.79	1.61
5 McDaniel et al. (2003)	A709 Gr. 50	Built-up I-section	TYPE 1	0.82	53.4	51.3	77.2	72.1	6.7	30.8	1.61	1.02	0.63	0.082	1.83	1.66
			TYPE 3	0.58	53.4	51.3	77.2	72.1	6.7	30.8	1.61	0.80	0.50	0.108	1.94	1.76
6 Gulec et al. (2012)	A709 Gr. 50	Built-up I-section	Spec. 1	1.11	53.0	53.0	78.3	81.9	6.2	35.5	2.25	1.58	0.70	0.076	1.77	1.57
			Spec. 2	1.11	53.8	53.0	82.7	81.9	6.2	35.5	2.25	1.58	0.70	0.076	1.87	1.66
7 Chi and Uang (2000)	A572 Gr. 50	Built-up I-section	SDE-1	0.64	57.1	58.4	87.3	79.5	4.4	50.0	3.00	1.43	0.48	0.124	1.75	1.58
			SDE-2	0.64	57.1	58.4	87.3	79.5	4.4	50.0	3.00	1.43	0.48	0.098	1.71	1.55
			SDE-3	0.86	57.0	58.4	88.5	79.5	6.9	50.7	2.67	1.27	0.48	0.081	1.65	1.49

<sup>a</sup> based on  $V_p = 0.6F_{yb}(d-2t_f)t_w$

<sup>b</sup> based on  $V_p = 0.6F_{yb}d t_w$

study. (Rolled wide-flange shapes of A36 steel are practically unavailable in the United States after the Northridge earthquake.) For built-up links, only A572 Gr. 50 steel and A709 Gr. 50 steel were considered. Note in Table 1 that  $h$  for computing  $h/t_w$  is defined in AISC 341: (1) the clear distance between flanges less the fillet or corner radius for rolled shapes or (2) the clear distance between flanges for welded built-up sections.

Okazaki and Engelhardt (2007) reported test results of 37 link specimens of A992 steel with five different W-shapes and varying lengths. One objective of the study was to investigate the effect of using different test loading protocols. Group 1 in Table 1 contains five short specimens with  $\rho < 1.5$  that were tested with the loading protocol consistent with that specified in the 2016 edition of AISC 341. (The majority of the specimens were tested with more severe loading sequences, which would potentially affect the failure mode and the associated overstrength, and thus they were excluded from the database.)

Group 2 includes 2 of 13 specimens reported by Mansour et al. (2011) in a study to develop replaceable links. Nine specimens that were excluded from the database were composed of back-to-back double channels that were bolted at both ends. The remaining four specimens used W-shape links with welded end plates at both ends. But tensile coupon tests were not conducted on two specimens, and therefore, they were excluded from the database because the actual overstrength could not be calculated.

Group 3 contains one of five specimens reported by Dusicka et al. (2010); three specimens that were excluded explored the potential of using low-yield steel and without intermediate stiffeners. A709 steel was specified for the remaining two specimens, one with Gr. 50 and another with Gr. 70 steel. Because the minimum specified yield stress of Gr. 70 steel violates the maximum value permitted in AISC 341, only one specimen (C345) was included in the database.

Group 4 includes two links reported by Itani et al. (2003). These two built-up links used A709 Gr. 50 steel. Relative to the web thickness, the flanges were the thickest among all specimens in the database ( $t_f/t_w = 4.0$  and  $3.0$ , respectively).

Group 5 consists of two large-size built-up links (depth = 37.4 in.) with A709 Gr. 50 steel (McDaniel et al., 2003). The  $t_f/t_w$  ratio (= 1.61) falls in the normal range of rolled shapes (e.g., see Group 1). Group 6 also includes two large-size links (depth = 40 in.) with the same grade of steel (Gulec et al., 2012). But the  $t_f/t_w$  ratio (= 2.25) is higher.

Three link specimens in Group 7 were tested to verify the cyclic performance of a coupled moment-resisting frame system, where vertical links were installed between two girders in a frame (Chi and Uang, 2000). A572 Gr. 50 steel was specified for the built-up links. The  $t_f/t_w$  ratio varies from 2.67 to 3.0.

Figure 1 shows the distribution of the link overstrength,  $\Omega_l$ , with respect to the normalized link length,  $\rho$ . The data is scattered within the range considered ( $\rho \leq 1.6$ ). But a trend does indicate that the link overstrength increases when  $\rho$  is reduced. Data points with rolled-shape links are circled; they show a lower overstrength ( $\Omega_l < 1.6$ ). Figure 2 shows similar plots with respect to the width-to-thickness ratios of the flanges and web. No clear trend can be observed between  $\Omega_l$  and these two width-thickness ratios.

AISC 341 Commentary (AISC, 2016) provides a reminder to the designers that a much higher overstrength may exist in built-up links with very thick flanges and very short lengths ( $\rho < 1.0$ ). To examine this effect, Figure 3 shows the distribution of  $\Omega_l$  with respect to two parameters: the ratio between the flange thickness and web thickness,  $t_f/t_w$ , and the ratio between the flange area and web area, with the latter being computed as  $(d - 2t_f)t_w$ . Contrary to that described in AISC 341, Figure 3 does not support the claim that thicker flange or larger flange area would necessarily produce a high overstrength factor.

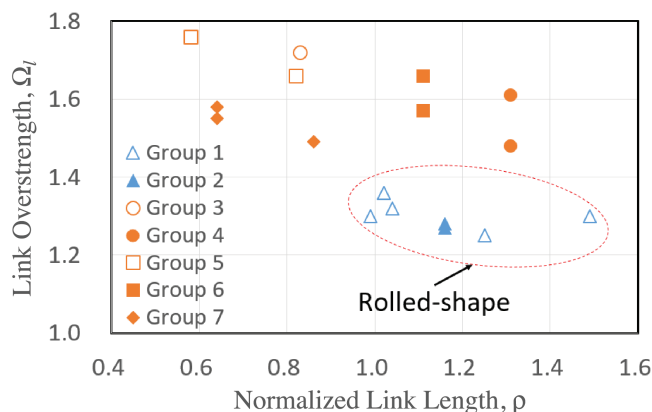


Fig. 1. Distribution of  $\Omega_l$  with respect to  $\rho$ .

A shear link under large inelastic deformations will cause flanges to kink at both ends of the link, a behavior that is analogous to the panel zone shear deformation in special moment frames. AISC *Specification*, ANSI/AISC 360 (AISC, 2022b), hereafter referred to as AISC 360, Section J10.6 provides an equation to compute the nominal shear strength of the panel zone in a beam-to-column moment connection. The equation is written in a slightly different form:

$$V_n = 0.60F_y d_c t_w (1 + K_w) \quad (4)$$

where

$$K_w = \frac{3b_{cf}t_{cf}^2}{d_b d_c t_w} \quad (5)$$

The  $K_w$  factor represents the contribution from localized bending (i.e., kinking) of the column flanges when the shear deformation reaches four times the shear yield strain of the panel zone. Because both panel zones in a special moment

frame and shear links in an EBF undergo large shear deformations, it was speculated that the link overstrength may also be related to  $K_w$ . When applying Equations 4 and 5 to the link,  $d_c$ ,  $b_{cf}$ ,  $t_{cf}$ ,  $t_w$ , and  $d_b$  are the depth, flange width, flange thickness, web thickness, and length of the link, respectively. Note that  $K_w$  can be rewritten as

$$K_w = \frac{12Z_f}{v_w} \quad (6)$$

where  $Z_f$  is the plastic section modulus of one flange,

$$Z_f = \frac{b_f t_f^2}{4} \quad (7a)$$

and  $v_w$  is the overall volume of the link web,

$$v_w = e d_c t_w \quad (7b)$$

Equations 6 and 7 show that not only a larger flange, but also a reduced web area,  $d_c t_w$ , and a shorter link length,  $e$ , will increase the value of  $K_w$ . Figure 4 shows the distribution

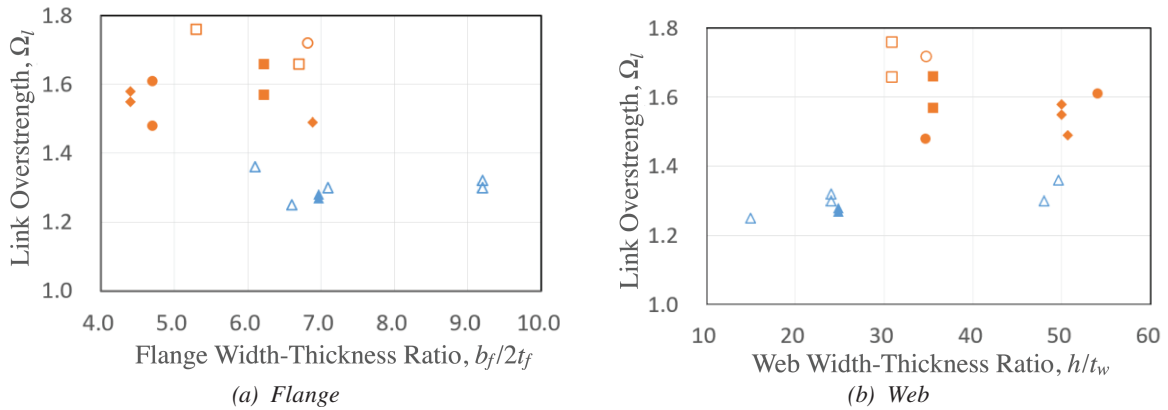


Fig. 2. Distribution of  $\Omega_l$  with respect to section width-thickness ratios.

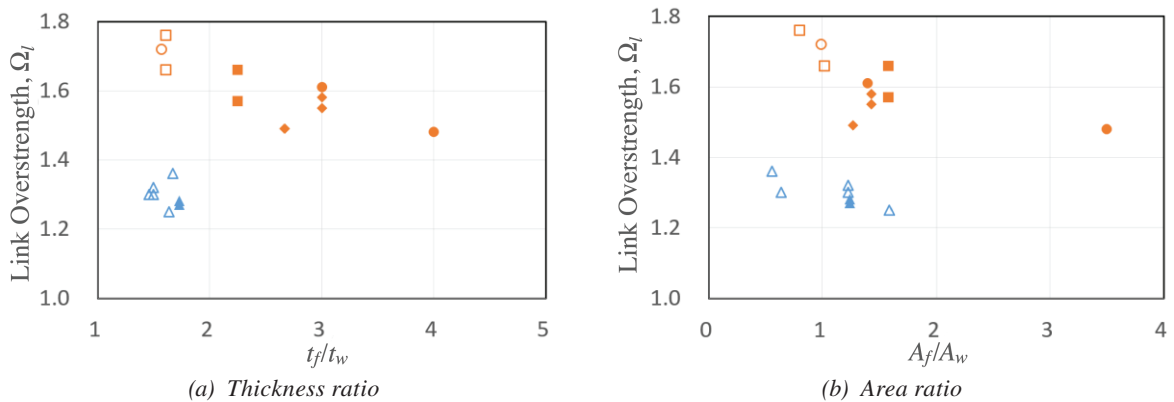


Fig. 3. Distribution of  $\Omega_l$  with respect to flange-to-web thickness and area ratios.

of the test data in the  $(1 + K_w)$  versus  $\Omega_l$  domain. Although the data is scattered, it appears to show that a larger contribution of the flanges due to kinking tends to produce a higher link overstrength. For the data collected, the figure also shows that built-up links tend to have a larger  $(1 + K_w)$  value.

Figure 5 uses the  $F_{ua}/F_{ya}$  ratio of the web for the plot, where  $F_{ya}$  and  $F_{ua}$  are the measured yield stress and tensile strength, respectively. Unlike all the previous parameters examined, this material strength ratio does show a stronger correlation with the link overstrength. This figure also shows that built-up links in the database have higher  $F_{ua}/F_{ya}$  ratios than those of rolled-shape links.

As mentioned in the literature review, finite element simulation by Barecchia et al. (2006) indicated that the overstrength factor would increase with an increase of the  $b_f/d$  ratio. Figure 6 shows the distribution of the link overstrength with respect to  $b_f/d$ . No clear trend can be observed. The observations from figures presented earlier are then used to guide the regression analysis.

## REGRESSION ANALYSIS

Parameters listed in Table 1 were considered in a multivariate regression analysis to establish an expression for predicting the link overstrength,  $\Omega_l$ . A sensitivity study showed that  $F_{ua}/F_{ya}$  of the web and  $(1 + K_w)$  have the most significant influence. Note that  $\Omega_l$  is based on the measured yield stress of the web (see Equation 3), yet  $(1 + K_w)$  measures the increase of link shear strength due to the contribution from flanges. The  $(1 + K_w)$  term needs to be adjusted to  $(1 + K_w)(F_{yfa}/F_{ywa})$  in regression to account for the difference of measured yield stresses between the web and flanges.

A regression results in the following expression with a coefficient of determination,  $R^2$ , of 0.781:

$$\Omega_l = 1.402 \left[ (1 + K_w) \frac{F_{yfa}}{F_{ywa}} \right]^{1.144} \left( \frac{F_{ua}}{F_{ya}} \right)^{0.414} \quad (8)$$

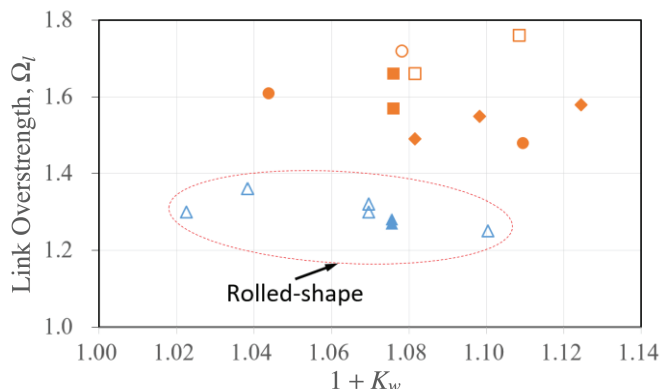


Fig. 4. Distribution of  $\Omega_l$  with respect to  $(1 + K_w)$ .

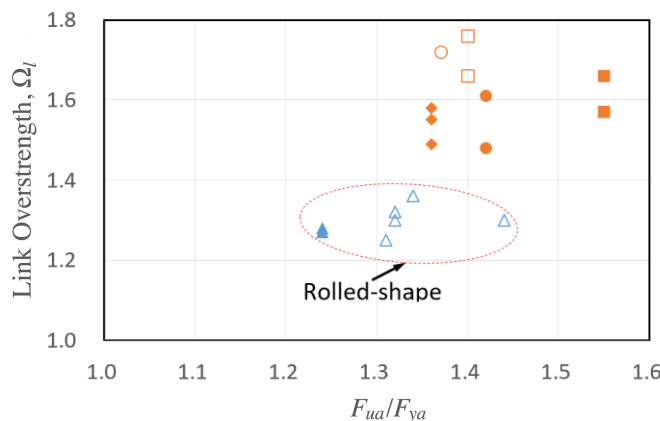


Fig. 5. Distribution of  $\Omega_l$  with respect to web  $F_{ua}/F_{ya}$  ratio.

Group No.	Specimen Designation	$(1+K_w) \frac{F_{yfa}}{F_{ywa}}$	$\left(\frac{F_{ua}}{F_{ya}}\right)^{0.5}$	$\Omega_t$	
				Equation 9	Test
1 Okazaki and Engelhardt (2007)	4A-RLP	1.00	1.15	1.57	1.45
	12-RLP	0.93	1.16	1.47	1.44
	8-RLP	0.94	1.20	1.55	1.37
	10-RLP	0.87	1.15	1.36	1.47
	S9	1.01	1.15	1.59	1.43
2 Mansour et al. (2011)	UT-3A	0.92	1.11	1.40	1.41
	UT-3B	0.92	1.11	1.40	1.42
3 Dusicka et al. (2010)	C345	1.13	1.17	1.81	1.90
4 Itani et al. (2003)	BU16	1.05	1.19	1.71	1.82
	BU30	0.99	1.19	1.61	1.79
5 McDaniel et al. (2003)	TYPE 1	1.12	1.18	1.82	1.83
	TYPE 3	1.15	1.18	1.86	1.94
6 Gulec et al. (2012)	SPEC. 1	1.08	1.24	1.83	1.77
	SPEC. 2	1.09	1.24	1.86	1.87
7 Chi and Uang (2000)	SDE-1	1.10	1.17	1.76	1.75
	SDE-2	1.07	1.17	1.72	1.71
	SDE-3	1.06	1.17	1.69	1.65

Table 2 lists the contribution of each of the last two terms on the right-hand side of Equation 8. Taking Specimen TYPE 3, for example, which is a large-size, full-scale built-up specimen with an overall link depth of 37.4 in. and a larger overstrength (1.94) from testing, each of these two terms (1.15 vs. 1.18) contribute comparably to the

overstrength. Specimen SPEC. 2, which is another large-size, full-scale built-up specimen with an overall link depth of 40 in. and a flange thickness of 2¼ in., has a larger contribution (1.24) from the  $F_{ua}/F_{ya}$  term, and the contribution from flange kinking is less (1.09). The small-size rolled-shape W16×36 link specimen 8-RLP also shows a large

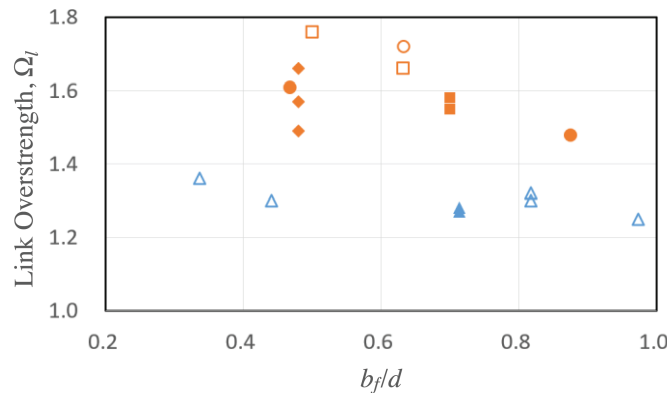


Fig. 6. Distribution of  $\Omega_t$  with respect to  $b_f/d$  ratio.

contribution (1.20) from the  $F_{ua}/F_{ya}$  term, but the contribution from the flange kinking is small (0.94), resulting in a smaller overall link overstrength. (The reason for a value of 0.94, which is smaller than 1.0, is because the measured yield stress of the flanges is smaller than that for the web.)

Equation 8 can be adjusted by rounding the exponents as follows ( $R^2 = 0.775$ ):

$$\Omega_l = 1.37 \left[ (1 + K_w) \frac{F_{yfa}}{F_{ywa}} \right] \left( \frac{F_{ua}}{F_{ya}} \right)^{0.5} \quad (9)$$

A comparison of the experimental and predicted overstrengths based on Equation 9 is shown in Figure 7(a). For code implementation in AISC 341,  $F_{ya}$  and  $F_{ua}$  for the web in Equation 9 can be replaced by  $R_y F_y$  and  $R_t F_u$ . Assuming that, for design, the expected yield stresses of the flange and webs are the same, Equation 9 becomes

$$\Omega_l = 1.37(1 + K_w) \sqrt{\frac{R_t F_u}{R_y F_y}} \quad (10)$$

where  $K_w$  is calculated using Equation 6, and  $F_y$  and  $F_u$  are the specified minimum yield and tensile strength of the web, respectively.

The  $\Omega_l$  expressions presented here are the link overstrength normalized by using the plastic shear strength defined in Equation 3; this strength is based on a web area of  $(d - 2t_f)t_w$  as defined in AISC 341. Because a web area of  $dt_w$  is used in AISC 360 (AISC, 2022b) instead, it is worthwhile to examine if using the following plastic shear strength to define the link overstrength would reduce the scatter of the data:

$$V_{pa} = 0.6 F_{ya} dt_w \quad (11)$$

Another regression results in the following with  $R^2 = 0.826$ :

$$\Omega_l = 1.3 \left[ (1 + K_w) \frac{F_{yfa}}{F_{ywa}} \right]^{1.165} \left( \frac{F_{ua}}{F_{ya}} \right)^{0.314} \quad (12)$$

Note that using Equation 11 to compute the link overstrength does reduce the scatter of the data somewhat. After simplification, the following expression can be used ( $R^2 = 0.814$ ):

$$\Omega_l = 1.23 \left[ (1 + K_w) \frac{F_{yfa}}{F_{ywa}} \right] \left( \frac{F_{ua}}{F_{ya}} \right)^{0.5} \quad (13)$$

Figure 7(b) shows the correlation with the test data. From Equation 13, the form suitable for design is:

$$\Omega_l = 1.23(1 + K_w) \sqrt{\frac{R_t F_u}{R_y F_y}} \quad (14)$$

## SUMMARY AND CONCLUSIONS

Eccentrically braced frames with short (or shear) I-shaped links are expected to perform better in a seismic event due to their high ductility capacity. But testing of short links in the past two decades showed that some links—especially those with built-up sections—exhibited a shear overstrength close to 2.0, significantly larger than the 1.5 observed in testing of rolled-shape links. For capacity design, such unusually

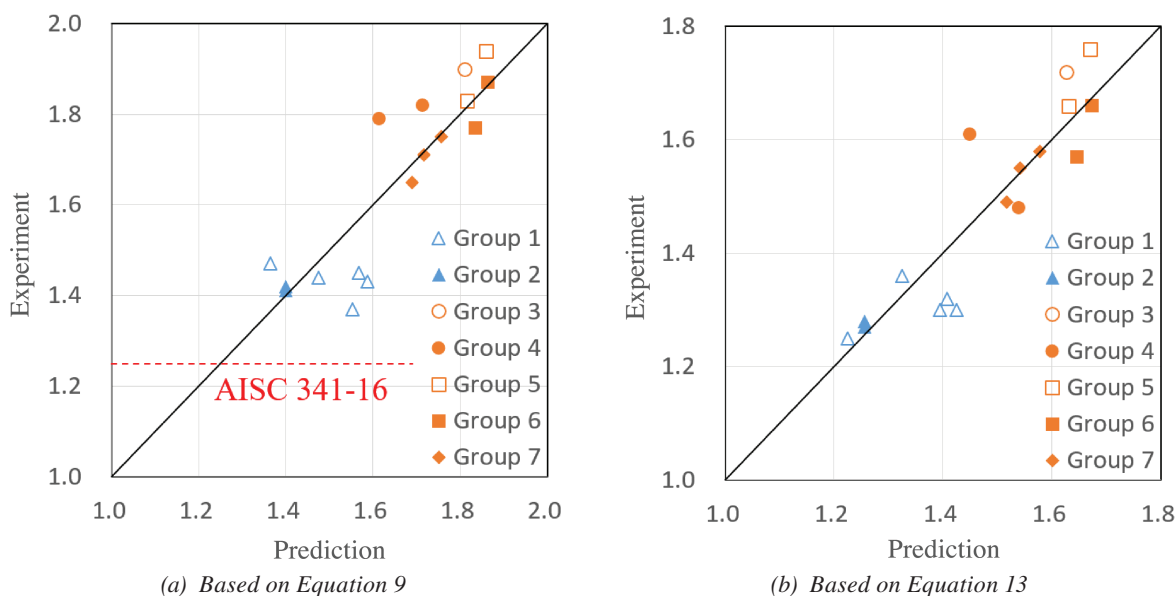


Fig. 7. Comparison of predicted and experimental overstrength factor.

high overstrength is also much larger than (1) the 1.25 factor for design of braces, columns, and gusset connections and (2) the 1.1 factor for design of beams outside the links stipulated in AISC 341, thus potentially leading to a mode of behavior inconsistent with the basis of EBF design. Although attempts have been made by some researchers in the past, no consensus could be reached on the main causes for the much higher overstrength. AISC 341 Commentary reminds designers to consider a high overstrength factor for large built-up links with very thick flanges and very short links. Still, no specific design guidance is provided.

This study addresses shear links only. An available experimental database for short links with both rolled and built-up sections and with Gr. 50 steel was assembled. A statistical evaluation was then conducted to identify key factors that contribute to high overstrength. It was found that a thick flange alone could not explain the high overstrength observed from testing. A multi-variate regression analysis was then conducted, and, for use in practical design, an equation (Equation 10) was proposed to evaluate the overstrength factor for shear links. The equation contains two contributing factors. The ratio between the expected tensile strength and expected yield stress of the web plays a more important role. The  $K_w$  term in Equation 10, which is defined in Equation 6, reflects the localized bending (or kinking) contribution of the flanges at link ends to the link shear strength; this effect is analogous to the column flange contribution of panel zone design strength in special moment frames.

#### ACKNOWLEDGMENTS

Part of this work was funded by the National Research Foundation of Korea (No. 2020R1A4A4079299).

#### REFERENCES

- AISC (1997), *Seismic Provisions for Structural Steel Buildings*, American Institute of Steel Construction, Chicago, Ill.
- AISC (2016), *Seismic Provisions for Structural Steel Buildings*, ANSI/AISC 341-16, American Institute of Steel Construction, Chicago, Ill.
- AISC (2022a), *Seismic Provisions for Structural Steel Buildings*, ANSI/AISC 341-22, American Institute of Steel Construction, Chicago, Ill.
- AISC (2022b), *Specification for Structural Steel Buildings*, ANSI/AISC 360-22, American Institute of Steel Construction, Chicago, Ill.
- Azad, S.K. and Topkaya, C. (2017), "A Review of Research on Steel Eccentrically Braced Frames," *Journal of Constructional Steel Research*, Vol. 128, pp. 5373.
- Barecchia, E., Della Corte, G., and Mazzolani, F.M. (2006), "Plastic Over-Strength of Short and Intermediate Links," *Proceedings of the 5th International Conference on Behaviour of Steel Structures in Seismic Areas (STESSA)*, pp. 177–183, Taylor & Francis Group, London.
- Bruneau, M., Anagnostopoulou, M., MacRae, G., Clifton, C., and Fussell, A. (2010), "Preliminary Report on Steel Building Damage from the Darfield Earthquake of September 4, 2010," *Bulletin of the New Zealand Society for Earthquake Engineering*, Vol. 43, No. 4, pp. 351–359.
- Bruneau, M., Uang, C.-M., and Sabelli, R. (2011), *Ductile Design of Steel Structures*, McGraw-Hill, New York, N.Y.
- Chi, B. and Uang, C.-M. (2000), "Cyclic Testing of Steel Shear Links for the San Francisco Moscone Convention Center Expansion Project," Report No. TR-99/06, Department of Structural Engineering, University of California, San Diego, La Jolla, Calif.
- Clifton, C., Bruneau, M., MacRae, G., Leon, R., and Fussell, A. (2011), "Steel Structures Damage from the Christchurch Earthquake Series of 2010 and 2011," *Bulletin of the New Zealand Society for Earthquake Engineering*, Vol. 44, No. 4, pp. 297–318.
- Dusicka, P., Itani, A.M., and Buckle, I.G. (2010), "Cyclic Behavior of Shear Links of Various Grades of Plate Steel," *Journal of Structural Engineering*, Vol. 136, No. 4, pp. 370–378.
- Ji, X.D., Wang, Y.D., and Okazaki, T. (2016), "Cyclic Behavior of Very Short Steel Shear Links," *Journal of Structural Engineering*, Vol. 142, No. 2, 04015114.
- Gulec, C.K., Gibbons, B., Chen, A., Sim, H.B., and Uang, C.-M. (2012), "Full-Scale Testing of Transbay Terminal Center Eccentrically Braced Frame Link Beams," *Proceedings of the 81st Annual Convention*, Structural Engineers Association of California, Sacramento, Calif., pp. 455–479.
- Itani, A.M., Elfass, S., and Douglas, B.M. (2003), "Behavior of Built-Up Shear Links under Large Cyclic Displacement," *Engineering Journal*, AISC, Vol. 40, No. 4, pp. 221–234.
- Kasai, K. and Popov, E.P. (1986), "General Behavior of WF Steel Shear Link Beams," *Journal of Structural Engineering*, Vol. 112, No. 2, pp. 362–382.
- Malley, J.O. and Popov, E.P. (1984), "Shear Links in Eccentrically Braced Frames," *Journal of Structural Engineering*, Vol. 110, No. 9, pp. 2,275–2,295.
- Mansour, N., Christopoulos, C., and Tremblay, R. (2011), "Experimental Validation of Replaceable Shear Links for Eccentrically Braced Steel Frames," *Journal of Structural Engineering*, Vol. 137, No. 10, pp. 1,141–1,152.

- McDaniel, C.C., Uang, C.-M., and Seible, F. (2003), "Cyclic Testing of Built-Up Steel Shear Links for the New Bay Bridge," *Journal of Structural Engineering*, Vol. 129, No. 6, pp. 801–809.
- Okazaki, T. and Engelhardt, M.D. (2007), "Cyclic Loading Behavior of EBF Links Constructed of ASTM A992 Steel," *Journal of Constructional Steel Research*, Vol. 63, No. 6, pp. 751–765.
- Popov, E.P. and Engelhardt, M.D. (1988), "Seismic Eccentrically Braced Frames," *Journal of Constructional Steel Research*, Vol. 10, pp. 321–354.
- Roeder, C.W. and Popov, E.P. (1978), "Eccentrically Braced Steel Frames for Earthquakes," *Journal of the Structural Division*, Vol. 104, No. 3, pp. 391–411.
- Richards, P.W. and Uang, C.M. (2006), "Testing Protocol for Short Links in Eccentrically Braced Frames," *Journal of Structural Engineering*, Vol. 132, No. 8, pp. 1,183–1,191.
- Sim, H.B. and Uang, C.-M. (2011), "Cyclic Testing of Shear Link Subassemblies in Support of Design for Transbay Transit Center in San Francisco," Report No. TR-11/02, Department of Structural Engineering, University of California, San Diego, La Jolla, Calif.